

# Direct Numerical Simulation of Turbulent Flows in an Eccentric Annulus Channel

Project Representative

Hisashi Ninokata Tokyo Institute of Technology

Authors

Hisashi Ninokata<sup>\*1</sup>, Tsunayuki Okumura<sup>\*1</sup>, Elia Merzari<sup>\*1</sup> and Takuma Kano<sup>\*2</sup>

\*1 Nuclear Engineering Department, Tokyo Institute of Technology

\*2 Japan Atomic Energy Research Institute

An attempt has been made to apply the direct numerical simulation (DNS) to a fully-developed single-phase turbulent flow analysis for an eccentric annulus channel configuration. The objective of this investigation is focused on the heterogeneity and local laminarization phenomena similar to those that prevail in the tight lattice rod bundle configurations. The DNS algorithm adopted here is based on the finite difference method being extended to the boundary-fitted coordinate system, verified for a number of numerical benchmarks and turbulent flows in flow channels of simple geometry, and can concentrate grids efficiently near the narrow gap boundary region. First a comparison between the DNS calculation and the numerical benchmark results by the spectral method has been made for flows in concentric annuli to demonstrate the accuracy of the DNS. Then the computations have been extended to a flow with the friction Reynolds number  $Re_\tau = 770$  in an eccentric annuli, first to get qualitative insights into the turbulent structure in reference to the experimental data available with higher friction Reynolds number  $Re_\tau = 1,440$ , and then to see the local laminarization near the narrow gap region.

**Keywords:** turbulent flow, anisotropy, DNS, eccentric annulus, secondary flow

## 1. INTRODUCTION

Liquid-metal-cooled fast reactors (LMFR) that are aimed at attaining high fuel burn-up and fuel breeding adopt the triangular fuel pin array configuration with the tight lattice pitch in order to increase the fuel-to-moderator ratio, thus to enhance the fuel utilization and extend the core life. In these options, it is necessary to evaluate the cladding temperature distribution and to identify the hot spot with high accuracy.

In the past, the direct numerical simulation (DNS) has been hardly applied to the turbulent flows inside a fuel pin bundle because of the computing power available to date. Therefore numerical estimation of detailed thermal hydraulics fields in pin bundles has been mainly carried out by the RANS (Reynolds Averaged Navier-Stokes model) approach ([1], [2], [3]). In general, however, it is often the case for the RANS turbulence models to fail in predicting secondary flows of the second kind, which is caused by the turbulence anisotropy and is supposed to have an important influence on the velocity and temperature profiles of the coolant in complex flow channel geometry. Furthermore the use of the wall function model substantially limits its applicability to these flows.

The present authors reported applications of the DNS code, SPARKLE-DNS that is based on the finite difference

method, extended to the boundary-fitted coordinate system [4]. To make the DNS more practical we eluded the difficulty with the compromise of renouncing calculation of the higher-order moments, e.g., skewness, flatness, etc., that swell the number of grids required for ensuring accuracy. Thus, we limited our estimations to the averaged velocity profile, second-order moments of turbulence, i.e., turbulence intensity, and Reynolds shear stress for deriving which we utilize the minimum number of grids necessary for ensuring requisite accuracy. In this work, this form of direct numerical simulation is carried out for turbulent flows in concentric as well as eccentric annuli. Calculation results are compared directly with numerical benchmark and indirectly in reference to experiment under a higher Re condition in order to verify that the method simulates turbulent fields accurately or reasonably. Moreover, results for local laminarization of turbulent flows are provided by the present simulations for an eccentric annulus flows near the narrow gap region.

## 2. COMPUTATIONAL PROCEDURE

### 2.1 Outline of the SPARKLE-DNS Code

The governing Navier-Stokes equations, extended to the boundary-fitted coordinate system [5] are the mass and the momentum conservation equations and a mean axial pres-

sure gradient is an input that drives incompressible flows through the flow channel. The numerical method is based on the fractional step method, with the collocated grid system. For the spatial derivatives, the second order accurate scheme is applied to the convection terms. The second order accurate central difference scheme for other terms while near the wall the viscous term is interpolated using inner three points. An explicit Adams-Bashforth scheme is used for the time-advancement of convection and diffusion terms. The Poisson-type pressure equation is solved by the scaling conjugate gradient method using FFT in the axial direction. The contravariant velocity components are transformed from the Cartesian velocity components by 4-point interpolation.

2.2 Computational Domain and Boundary Conditions

DNS calculations in this work are limited to two types of annulus channel and shown in Fig. 1. The concentric annulus channel flow conditions are the same as those of numerical benchmark provided by Seo et al. [6] and the eccentric annulus channel geometry is the same as that given by Nouri et al. [7] Non-slip condition is imposed on the wall surface, and a periodic condition is imposed at the flow inlet and outlet with the axial spacing of  $5 \times D_h$ .

In the calculations that will shown in the following, the ratio of radius of the inner circular column  $R_{in}$  to outer pipe  $R_{out}$  is 0.1 for the concentric annular channel and 0.5 for the eccentric annular channel. The eccentricity  $e = l/(R_{out} - R_{in})$  is 0.5 where  $l$  is the distance between two centers of two circles of the eccentric annuli.

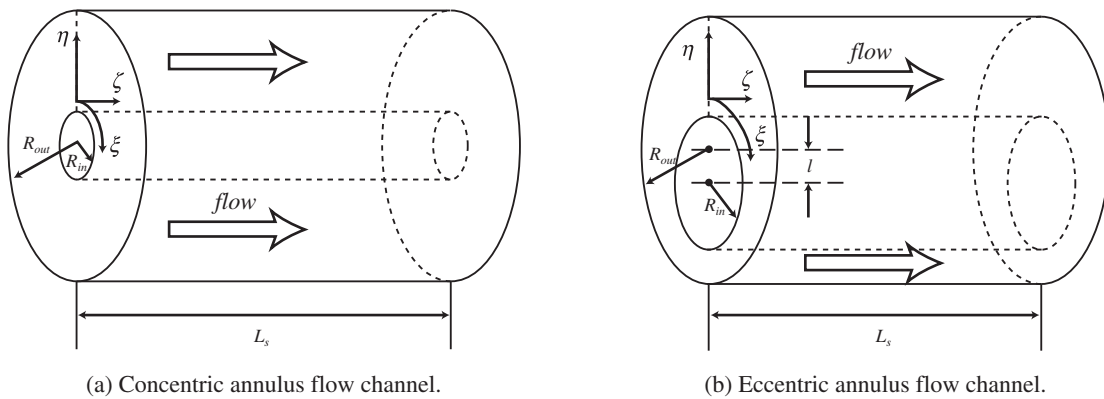


Fig. 1 Flow channel geometry.

Table 1 Calculation conditions.

Channel geometry		$Re_\tau$	# of grids		Grid sizes		$\Delta t^+$
			$\xi$	$\eta$	$\Delta x^+$	$\Delta y^+$	
Concentric Annulus	$R_{in} = 0.05555 D_h$ $R_{out} = 0.55555 D_h$	570	$\xi$	256	$\Delta x^+$	7.8 ~ 0.8	1.2E - 4
			$\eta$	64	$\Delta y^+$	1.0 ~ 16.7	
			$\zeta$	192	$\Delta z^+$	14.8	
Eccentric Annulus	$R_{in} = 0.497525 D_h$ $R_{out} = 0.997525 D_h$ $l = 0.25 D_h$	770	$\xi$	384	$\Delta x^+$	6.3 ~ 12.6	1.0E - 4
			$\eta$	112	$\Delta y^+$	1.0 ~ 9.1	
			$\zeta$	336	$\Delta z^+$	11.5	

3. RESULTS

3.1 Computational Cases

Table 1 shows calculation conditions for both channel geometries. Simulations of the flows of friction Reynolds number  $Re_\tau = 570$  and 830 in the concentric and eccentric annuli, respectively, have been carried out, each corresponding to the bulk Reynolds numbers 8,400 and 12,100. The fully-developed turbulent flow is identified by the fact that the sample data of the averaged turbulent energy, bulk velocity, and wall shear stress show statistically a steady-state. The instantaneous velocities obtained by the present simulation are time-averaged and space-averaged in the axial direction.

3.2 Comparison of the Results with Spectral Method

Agreement of DNS by the SPARKLE-DNS code and the benchmark results by the spectral method due to Seo, et al. [6] has been excellent for the concentric annulus flow. Figures 2 and 3 show, for example, comparisons of the axial flow velocity profile plotted from the inner wall and r.m.s. of the velocity fluctuations in the circumferential direction.

3.3 Turbulent Flow Fields in an Eccentric Annulus Channel

It is noted that the calculated flow field in the eccentric channel has not yet been stabilized in the reporting period. It is due to insufficient computing time: i.e., the time for ensemble average is 11.2 while it was 54.6 for the concentric annulus flow case. Figure 4 shows an instantaneous axial velocity distribution. It is not as symmetric as it should be

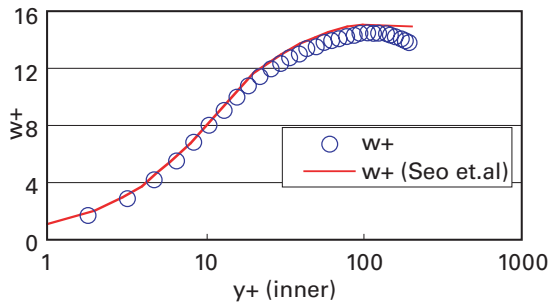


Fig. 2 Axial velocity profile.

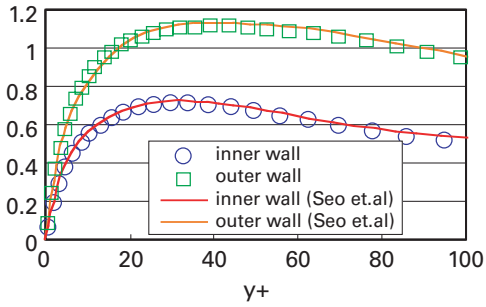


Fig. 3 Velocity fluctuations in the circumferential direction.

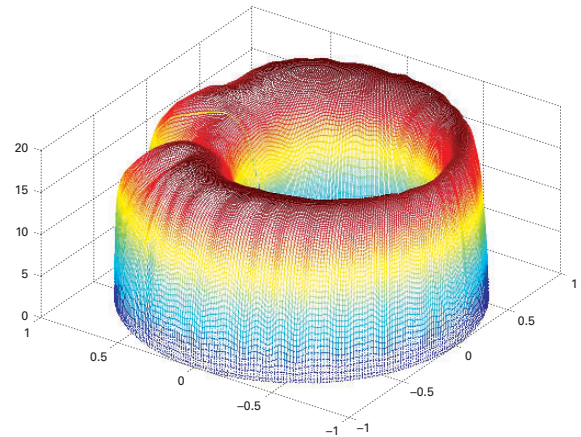


Fig. 4 Axial velocity distribution.

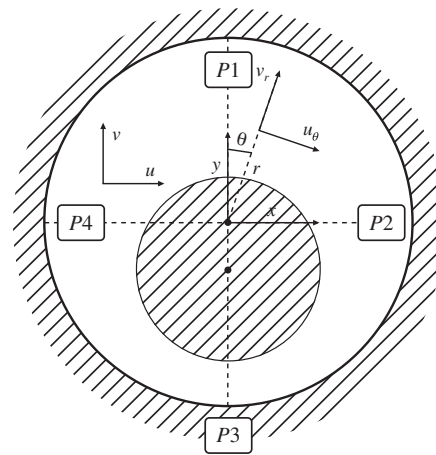


Fig. 5 Location of the lines P1 to P4.

with distortions in the wider gap region. A secondary flow distribution is indicating that the turbulence heterogeneity is strong and the vortex pattern fluctuates time to time. Nevertheless, the calculation results provide us many physical insights and are described briefly in the following.

Figure 5 locates the lines along which computed results will be compared to measurement from the experiment by Nouri [7] of which the friction Reynolds number for a comparison is almost twice as high as that of the calculation.

Figures 6 and 7 shows comparisons between calculation and experiment for axial flow velocity profiles along the widest and narrowest gap positions, i.e., P1 and P3 (see Fig. 5 for the positions). The comparisons are not direct because Reynolds number of the DNS calculation is a half of that of experiment as noted before. As shown in Fig. 7, the profile along P3 suggests that the laminarization effects prevail in the narrow gap region. This transition is shown also by Fig. 8 that exhibits more contributions of molecular viscosity to the total Reynolds shear stress along the narrowest gap near the wall boundary than in the rest of wider gap region. Figure 9 shows a distribution of the local Reynolds number ( $Re_{local}$ ) in the azimuthal direction where  $Re_{local}$  is based on the averaged velocity along a line normal to the outer surface of inner circular column of the annulus, and on the line length to the inner wall of the outer circular tube. The figure suggests that, even if the overall flow Reynolds number is in a fully turbulent flow regime ( $Re_{bulk} = 12,000$ ), the flow starts showing a typical behavior of laminarization near the narrow gap region where  $Re_{local}$  is around 4,000. In fact, the velocity profile has been found to coincide with that of the Couette-Poiseuille's flow regime near the wall. A deviation

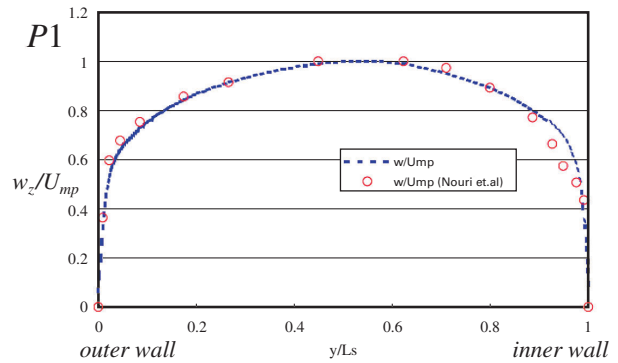


Fig. 6 Axial velocity profile along P1 line.

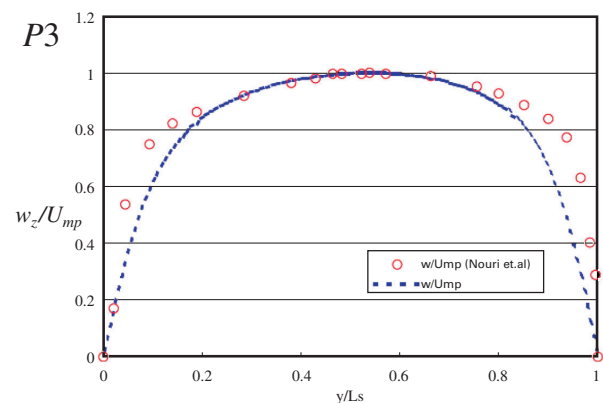


Fig. 7 Axial velocity profile along P3 line.

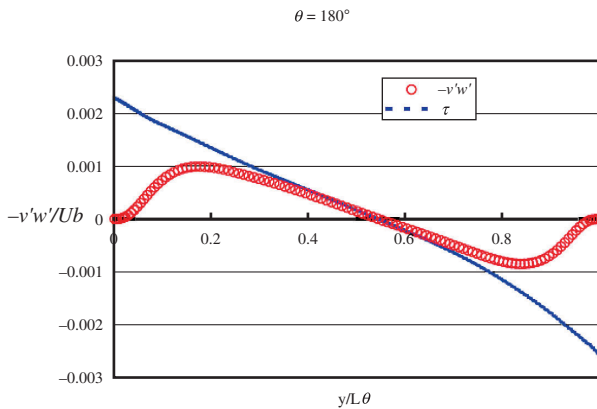


Fig. 8 Reynolds shear stress distribution along P3 line.

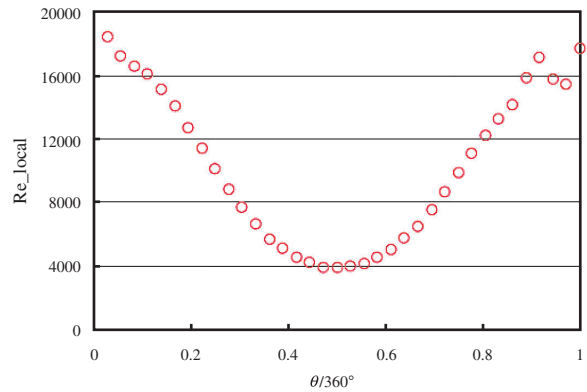


Fig. 9 Local Reynolds number distribution.

from the laminar flow regime in the turbulent core region is caused by the turbulence transport by the secondary flows and will be assessed in more details in the next stage of the work that continues.

#### 4. CONCLUDING REMARKS

In this work, DNS has been carried out to investigate turbulent flow characteristics in simpler geometry than the pin bundle. Even if the calculations were done on two nodes of the Earth Simulator, DNS results are extremely useful in obtaining physical insights into the complicated local turbulence structure observed in flows in nuclear fuel pin bundles. It is true in particular for low Reynolds number turbulent flows where experimental data are not or less available.

It is planned that the calculation should be continued on for the eccentric annulus channel flows to confirm the fully developed flow condition and flow stabilization, and then establish turbulence flow data base that should be useful for engineering applications. The targeted phenomena include the local laminarization and global pulsation phenomena. There influences of the anisotropic turbulence structure and eddy migration behaviors in the non-uniform flow channels will be investigated in detail and feed back to SGS modeling of LES will be carried out.

#### REFERENCES

1. Rapley, C.W., Gosman, A.D., 1986. The prediction of fully developed axial turbulent flow in rod bundles, *Nucl. Eng. Des.*, **97**, pp.313–325
2. Lee, K.B., Jang, H.C., 1997. A numerical prediction on the turbulent flow in closely spaced bare rod arrays by a nonlinear  $k-\varepsilon$  model, *Nucl. Eng. Des.*, **172**, pp.351–357
3. Baglietto, E. and Ninokata, H., 2004. CFD modeling of secondary flows in fuel rod bundles, N6P363, 6<sup>th</sup> Int. Top. Mtg on Nuclear Reactor Thermal Hydraulics, Operations and Safety (NUTHOS-6), Nara.
4. Ninokata, H., et al, 2005. Direct numerical simulation of turbulent flows in subchannels of a tight lattice bundle, *Annual Report of the Earth Simulator Center*, pp.293–297.
5. Zhang, Y., Street, R.L., and Koseff, J. R., 1994. A non-staggered grid, fractional step method for time-dependent incompressible Navier-Stokes equation in curvilinear coordinates", *J. Comput. Phys.*, **114**, pp.18–33
6. Seo Y., Gwang H., Hyung J., 2002. Direct numerical simulation of turbulent concentric annular pipe flow Part 1: Flow field, *International Journal of Heat and Fluid Flow* **23**.
7. Nouri, J.M., Umur, H., Whitelaw, J.H., 1993. "Flow of Newtonian and non-Newtonian fluids in concentric and eccentric annuli", *J. Fluid Mech.* vol.253, pp.617–641.

# 直接乱流シミュレーションによる偏心二重円環流路内の乱流評価

プロジェクト責任者

二ノ方 寿 東京工業大学大学院原子核工学専攻

著者

二ノ方 寿<sup>\*1</sup>, 奥村 剛征<sup>\*1</sup>, Elia Merzari<sup>\*1</sup>, 叶野 琢磨<sup>\*2</sup>

\*1 東京工業大学大学院

\*2 日本原子力研究所

本研究の目的は、流路チャンネルが複雑で実験計測上取得困難な乱流特性などを高い信頼性の裏づけをもったDNSによって提供し、現象の解明を実施するとともに現象の機構論的なモデル化を行って工学的な応用に有効に活用することである。

複雑形状流路の典型である高速炉または低減速型軽水炉炉心における稠密格子配列型燃料集合体サブチャンネル内の乱流構造のRe数依存性や配列格子のピッチ対燃料直径比に対する依存性は現象論的に極めて複雑である。その現象解明を行うには計算科学的手法が唯一の手段と考えられる。稠密格子燃料集合体内サブチャンネル内の乱流は、燃料要素間隔が狭いために壁の影響を強く受け、非等方性が強い。そのため、等方性乱流を仮定した $k-\varepsilon$ モデルや、壁関数を用いたモデルでは説明できない現象が多い。一般的に燃料集合体内の乱流は、 $P/D$ の減少およびRe数が低くなると燃料間隙部近傍でその非均質性が増すとともに、局所的な乱流-層流遷移領域を含み、流れそのものが不安定となることが予測される。したがって、これらの予測を数値的に確認し、実験的に取得困難な乱流データを設計および安全評価へ提供することが重要となっている。

本研究においては、燃料集合体より簡略な流路形状である偏心二重円環流路内における十分に発達した乱流を対象として、境界適合型座標系上のDNSを実施した。まず、DNSの精度を確認するために実施した同心円環流路内乱流計算結果は、スペクトル法によるベンチマーク結果と、時間平均流速分布、各種乱流統計量の分布について一致することを示した。偏心二重円環流路内乱流(計算上 $Re = 12,000$ )については、より高いRe数( $= 24,000$ )乱流実験データを参考にDNSから得られた結果の分析を実施し、狭隘ギャップでの局所的層流遷移の発現、および関連した低 $Re_t$ における各種統計量などに関する知見を得た。例えば狭隘部の近接壁近傍においては、平板流路の場合に示される直線状の全せん断応力分布からのずれが大きくなりレイノルズせん断応力が支配的となることなど、実験的には取得が困難なデータが得られている。とくに、特性長さを、内管外側表面法線方向の外管内側表面までの距離、平均流速を当該法線上で定義して得られる局所Re数は、最狭隘ギャップにおいて乱流から層流へ遷移する領域に入っていることを示唆しており、実際、壁際における流速分布はCouette-Poiseuille's流れそのものであることが示された。今後、燃料集合体内乱流と基本的に類似の挙動を示すと考えられる偏心二重円環内乱流について、より詳細な格子かつより長い軸方向距離をとりDNSを継続するとともにデータベース化を継続し、大渦シミュレーションのSGSモデル構築に資する。また、局所層流化現象と二次流れによる運動量輸送との関連、グローバルパルセーション現象の発現などをより定量的に把握するとともに、モデル化を実施する予定である。

キーワード : DNS, 乱流, 非等方性, 二次流れ, 偏心二重円環流路